Fermi systems with long scattering lengths

Henning Heiselberg
NORDITA, Blegdamsvej 17, DK-2100 Copenhagen Ø, Denmark
(Received 8 August 2000; published 14 March 2001)

Ground-state energies and superfluid gaps are calculated for degenerate Fermi systems interacting via long attractive scattering lengths such as cold atomic gases, neutron, and nuclear matter. In the intermediate region of densities, where the interparticle spacing ($\sim 1/k_F$) is longer than the range of the interaction but shorter than the scattering length, the superfluid gaps and the energy per particle are found to be proportional to the Fermi energy and thus differ from the dilute and high-density limits. The attractive potential increase linearly with the spin-isospin or hyperspin statistical factor such that, e.g., symmetric nuclear matter undergoes spinodal decomposition and collapses whereas neutron matter and Fermionic atomic gases with two hyperspin states are mechanically *stable* in the intermediate density region. The regions of spinodal instabilities in the resulting phase diagram are reduced and do not prevent a superfluid transition.

DOI: 10.1103/PhysRevA.63.043606 PACS number(s): 03.75.Fi, 05.30.Fk

I. INTRODUCTION

Dilute degenerate Fermi systems with long scattering lengths are of interest for nuclear and neutron star matter (see, e.g., [1]). Recently, also dilute systems of cold Fermionic atoms have been trapped [2]. The number density is sufficient for degeneracy to be observed and superfluidity is expected at critical temperatures similar to the onset of Bose-Einstein condensates, $\sim 10-100$ nK. *S*-wave scattering lengths can be very long, e.g.,[1] $a=-2160$ bohrs radii for triplet ^{6}Li and $a\sim 18.8$ fm for neutron-neutron interactions. These scattering lengths $|a|$ are much longer than the typical range of the potentials, respectively, $R\sim 1$ fm for strong interactions and $R\sim 10-100$ Å for van der Waals forces. Generally, when $|a|\gg R$, three density regimes naturally emerge: the low-density (or dilute, $k_F^{-1}\gtrsim|a|$), the high-density ($k_F^{-1}\lesssim R$), and the *intermediate density region* ($R\lesssim k_F^{-1}\lesssim|a|$).

The latter region of densities is the object of study here. It will be shown that previous conjectures based on extrapolations from the dilute limit fail. Instead it is found that both the energy per particle and the superfluid gaps scale with the Fermi energy. They depend only on statistical factors but not on the scattering length, range, or other details of the interaction. Consequently, phase diagrams are dramatically altered and the stability criteria differ so that two spin systems are actually *stable*.

The paper is organized as follows. In Sec. II the scaling and poles of the effective scattering amplitude are studied in a homogeneous many-body system going from dilute to intermediate densities. In Sec. III the ground-state energies are calculated at intermediate densities and compared to well-known results from the dilute and high-density limits. In Sec. IV extensions to finite temperatures are discussed and a phase diagram is constructed displaying regions of superfluidity and spinodal instabilities. In Sec. V the properties of finite systems of Fermions are investigated as they are relevant for current experiments with magnetically trapped cold atoms. Finally, a summary and conclusion is given.

II. THE EFFECTIVE SCATTERING AMPLITUDE AND SUPERFLUIDITY

Consider a homogeneous many-body system of fermions of mass m at density, $\rho=\nu k_F^3/6\pi^2$, where ν is the statistical factor, e.g., $\nu=4$ for symmetric nuclear matter and $\nu=2$ for neutron matter as well as for the ^{40}K atomic gas with two hyperspin states currently studied at JILA [2]. The scattering lengths and Fermi momentum k_F are assumed the same for all spin-isospin-hyperspin components in the system but interesting effects of varying the relative densities of the various components will be discussed at the end. Particles are assumed to be nonrelativistic and to interact through attractive two-body contact interactions. The details of the potential are not important, only its range $\sim R$ and scattering length a. We shall be particularly interested in cases where $R\ll|a|$, which occur when, for example, the two-body potential can almost support a bound state or resonance.

At dilute or intermediate densities the particles interact via short-range interactions that appear singular on length scales of the order of the interparticle distance $\sim k_F^{-1}$. Such systems are best described by resumming the multiple interactions in terms of the scattering amplitude. The Galitskii integral equations [3] for the effective two-particle interaction or scattering amplitude in the medium are given by the ladder resummation

$$\Gamma(\mathbf{p},\mathbf{p}',\mathbf{P})=\Gamma_0(\mathbf{p},\mathbf{p}',\mathbf{P})+m\sum_{\mathbf{k}}\Gamma_0(\mathbf{p},\mathbf{k},\mathbf{P})\times\left[\frac{N(\mathbf{P},\mathbf{k})}{\kappa^2-k^2}-\frac{1}{\kappa^2-k^2}\right]\Gamma(\mathbf{k},\mathbf{p}',\mathbf{P}). \quad (1)$$

Here, $\Gamma_0=4\pi a/m$ is the *s*-wave scattering amplitude in vacuum; the total energy of the pair in the center of mass is κ^2/m; $\mathbf{p},\mathbf{k},\mathbf{p}'$ are the relative momentum of the pair of interacting particles in the initial, intermediate, and final states,

[1]The sign convention of negative scattering length for attractive potentials is used. Also $\hbar=c=1$.

respectively, and **P** the total momentum; $N(\mathbf{P},\mathbf{k})=+1$ for particle-particle propagation ($|\mathbf{P}\pm\mathbf{k}|\geqslant k_F$), $N(\mathbf{P},\mathbf{k})=-1$ for hole-hole propagation ($|\mathbf{P}\pm\mathbf{k}|\leqslant k_F$), and zero otherwise. For spin independent interactions the amplitudes contain a factor $(1-\delta_{\nu_1\nu_2})$ that takes exchange into account between identical spins $\nu_1=\nu_2$.

For obtaining BCS gaps it is sufficient to study pairs with $\mathbf{P}=0$ where Eq. (1) is simply

$$\Gamma=\Gamma_0+2m\sum_{k\leqslant k_F}\Gamma_0\frac{1}{\kappa^2-k^2}\Gamma. \tag{2}$$

Note the factor of 2 due to particle-particle and hole-hole propagation each contributing by the same amount in nondense systems. The ladder resummation implicit in Eq. (1) insures that only momenta smaller than Fermi momenta enter. Γ_0 varies on momentum scales $\sim 1/R\gg k_F$ only and can therefore be considered constant at low and intermediate densities. Equation (2) is then easily solved for momenta near the Fermi surface

$$\Gamma=\Gamma_0\left[1-\frac{2}{\pi}k_Fa\left(2+\frac{\kappa}{k_F}\ln\frac{k_F-\kappa}{k_F+\kappa}\right)\right]^{-1}. \tag{3}$$

The in-medium scattering amplitude has a pole due to Cooper pairing when

$$\Delta\equiv\frac{k_F^2-\kappa^2}{m}=\frac{(k_F+\kappa)^2}{m}\exp\left(\frac{\pi}{2\kappa a}-2\frac{k_F}{\kappa}\right)$$
$$\simeq E_F\frac{8}{e^2}\exp\left(\frac{\pi}{2k_Fa}\right),\quad k_F|a|\ll 1, \tag{4}$$

where $E_F=k_F^2/2m$ is the Fermi energy. The critical temperature is $T_c=(\gamma/\pi)\Delta$, where $\gamma=e^C$ and $C=0.577$ is Euler's constant. Equation (4) is the BCS gap in the dilute limit, which agrees with gaps calculated in Ref. [4].

However, Gorkov and Melik-Barkhudarov [5] showed that spin fluctuations lead to a higher-order correction $\sim(k_Fa)^2$ in the denominator of Eq. (3) that is amplified by logarithmic terms $\sim\ln(\Delta)\sim 1/k_Fa$. It contributes by a (negative) constant in the exponent and leads to a reduction of the gap in the dilute limit by a factor $(4e)^{1/3}=2.215\ldots$ as compared to Eq. (4) for two spins. Generally for ν spins, isospins, or hyperspins the gap is [6]

$$\Delta=E_F\frac{8}{e^2}(4e)^{\nu/3-1}\exp\left[\frac{\pi}{2ak_F}\right]. \tag{5}$$

In the intermediate density region pairing must still occur since the interaction is attractive. The validity of the expressions of Eqs. (4) and (5) in this density regime will be discussed further below. They predict that in the limits $a\to-\infty$ and $R\to 0$ the gap cannot depend on either a, R, or other details of the potential. For dimensional reasons the gap can therefore only be proportional to the Fermi energy.

III. GROUND-STATE ENERGIES

The ground-state energy is another crucial property of the system. In terms of the on-shell effective scattering amplitude it is [3,7]

$$E=\sum_{k_1\nu_1}\frac{k_1^2}{2m}+\frac{1}{2}\sum_{k_1k_2\nu_1\nu_2}\Gamma(\mathbf{p},\mathbf{p},\mathbf{P})(1-\delta_{\nu_1\nu_2})$$
$$=\frac{3}{5}\frac{k_F^2}{2m}N+\frac{\nu(\nu-1)}{2}\sum_{k_1k_2}\Gamma(\mathbf{p},\mathbf{p},\mathbf{P}). \tag{6}$$

Here, $N=V\rho$ is the number of particles and the summations ν_1,ν_2 include spin and isospin or hyperspin states. The factor $(1-\delta_{\nu_1\nu_2})$ in the amplitude due to exchange, has now been written explicitly. Antisymmetrization of the wave function prevents identical particles from being in relative s states. At low and intermediate densities, $k_FR\ll 1$, the exchange term is $1/\nu$ of the direct one for spin independent interactions.

Before investigating the intermediate density region, a brief review of results at low and high densities is given.

A. Low densities (dilute): $k_F|a|\ll 1$

At low densities, $k_F|a|\ll 1$, gaps are small and have little effect on the total energy of the system. Expanding the effective scattering amplitude of Eq. (1) in the small quantity k_Fa, the energy per particle is obtained from Eq. (6) by summing over momenta of the two interacting particles

$$\frac{E}{N}=E_F\left\{\frac{3}{5}+(\nu-1)\frac{2}{3\pi}k_Fa+(\nu-1)\frac{4(11-2\ln 2)}{35\pi^2}\right.$$
$$\left.\times(k_Fa)^2+\mathcal{O}((k_Fa)^3)\right\}. \tag{7}$$

It consists of, respectively, the Fermi kinetic energy, the standard dilute pseudopotential [8] proportional to the scattering length and density, and orders $(k_Fa)^2$ [9] and higher [10].

At zero temperature the hydrodynamic sound speed squared can, at low temperatures, be expressed as

$$s^2=\frac{1}{m}\left(\frac{\partial P}{\partial\rho}\right)=\frac{1}{m}\frac{\partial}{\partial\rho}\left(\rho^2\frac{\partial E/N}{\partial\rho}\right). \tag{8}$$

With the energy per particle of Eq. (7) at low densities, the sound speed can be expanded as

$$s^2=\frac{1}{3}v_F^2\left[1+\frac{2}{\pi}(\nu-1)k_Fa+\cdots\right], \tag{9}$$

where $v_F=k_F/m$ is the Fermi velocity. It is commonly conjectured from the first two orders that the Fermion (and Bose) gases undergo spinodal instability when the sound speed squared becomes negative, which occurs when $k_Fa\lesssim-\pi/2(\nu-1)$. However, at the same densities, the dilute

approximation leading to Eq. (7) fails and so does the conjecture as will be shown below.

B. High densities, $k_F R \gg 1$

At high densities, $k_F R \gtrsim 1$, the particle potentials overlap and each particle experience on average the volume integral of the potentials. The energy per nucleon consists of the Fermi kinetic energy and the Hartree-Fock potential [see, e.g., [7], Eq. (40.14)]:

$$\frac{E_{HF}}{N} = \frac{3}{5}E_F + \frac{\rho}{2}\int d^3 r V(r)\left[1 - \frac{1}{\nu}\left(\frac{3j_1(rk_F)}{rk_F}\right)^2\right]. \quad (10)$$

The latter term is the exchange energy, which vanishes at very high densities, $k_F R \sim R/r_0 \gg 1$, leaving the Hartree potential term only. At lower densities, $k_F R \sim R/r_0 \ll 1$, it is identical to the first integral, i.e., the Hartree direct term is ν times the Fock exchange term as also found in the dilute limit, Eqs. (7)–(11).

As shown in Ref. [11], the Hartree potential is considerably less attractive than the dilute potential. In fact it vanishes when the range of the interaction goes to zero and the scattering length to infinity. Take for example a square-well potential of range R and depth $-V_0$. Long scattering lengths require $V_0 R^2 \to \pi^2/4m$, and therefore the Hartree potential is $\propto V_0 R^3 \sim R \to 0$. Only in the Born approximation do the Hartree (10) and dilute potentials (7) coincide since the Born scattering length is $a_{Born} = (m/4\pi)\int d^3 r V(r)$.

Short-range repulsion complicates the high-density limit. In nuclear and atomic systems the repulsive core is only of slightly shorter range than the attractive force. It makes the liquid strongly correlated and the Hartree-Fock approximation fails [12,7]. How the short-range repulsion turns the attraction to repulsion at these even higher densities will, however, not affect the intermediate density region.

C. Intermediate densities, $|a| \gg k_F^{-1} \gg R$

At intermediate densities, $|a| \gg k_F^{-1} \gg R$, the scattering length expansion in Eq. (7) breaks down. Brueckner and Bethe and Goldstone [12] pioneered such studies for nuclear matter and ^{3}He where the range of interactions, scattering lengths, and repulsive cores all are comparable in magnitude. In our case the range of interaction is small, $k_F R \ll 1$, and therefore all particle-hole diagrams are negligible. Higher-order particle-particle and hole-hole diagrams do contribute by orders of $\sim \Gamma_0 (m k_F \Gamma)^n$. It is evident from Eq. (4) that at intermediate densities Γ no longer is proportional to Γ_0 or the scattering length but instead $\Gamma \propto (m k_F)^{-1}$. Due to the very restricted phase space such higher-order terms are usually neglected as in standard Brueckner theory. This truncation is similar to the Padé approximation. Γ of Eq. (1) can therefore be considered as a resummation of an important class of diagrams. The Cooper instability complicates the calculation of Γ. If the gap is small the instability occurs only for pairs near the Fermi system with opposite momenta and spin and the effect on the total energy is small. The momentum dependence of the effective scattering amplitude also complicates a self-consistent calculation. These complications can be dealt with by approximating Γ by its momentum average value in Eq. (1). The momentum integrals are then analogous to those in the dilute limit (7), and one obtains from Eq. (6)

$$\frac{E}{N} \simeq E_F\left[\frac{3}{5} + \frac{(\nu-1)\frac{2}{3\pi}k_F a}{1 - \frac{6}{35}\pi(11 - 2\ln 2)k_F a}\right]. \quad (11)$$

This expression is valid for dilute systems, where it reproduces Eq. (7), and approximately valid within the Galitskii ladder resummation at intermediate densities, $R \ll k_F^{-1} \ll |a|$, where it reduces to

$$\frac{E}{N} = E_F\left[\frac{3}{5} - (\nu-1)c_1\right] = E_F c_1(\nu_c - \nu), \quad (12)$$

with $c_1 = 35/9(11 - 2\ln 2) \simeq 0.40$ and $\nu_c = 1 + 3/5c_1 \simeq 2.5$. Both the attractive and the kinetic part of the energy per particle are proportional to the Fermi energy at these intermediate energies as found for the gaps above.

The other remarkable feature of Eq. (12) is that the energy per particle changes sign for a critical number of degrees of freedom, $\nu_c \simeq 2.5$. Fermi systems with more degrees of freedom such as symmetric nuclear matter have negative energy per particle and will therefore implode, undergo spinodal decomposition, and fragment [13]. Contrarily, systems with $\nu \lesssim \nu_c$ such as neutron matter and atomic systems with only two hyperspins have positive energy per particle and will therefore explode, if not contained. This is also evident from the sound speed squared, which from Eqs. (8) and (12) becomes

$$s^2 = (5/9)c_1(\nu_c - \nu)v_F^2. \quad (13)$$

Calculations for pure neutron matter and symmetric nuclear matter at low densities by variational Monte Carlo [1] and in neutron matter by Pade's approximants to R-matrix calculations [14] independently confirm the above results approximately in a limited range of intermediate densities. In the density range $\rho_0 \gtrsim \rho \gtrsim |a|^{-3} \simeq 10^{-4}\rho_0$ the energy per particle is positive for neutron matter and negative for symmetric nuclear matter [1]. They scale approximately with $\rho^{2/3}$ with coefficients compatible with Eq. (12). In symmetric nuclear matter the intermediate density regime is, however, limited since protons also interact through the triplet channel, which has a shorter repulsive scattering length $a_t \simeq 5.4$ fm, besides the singlet one, $a_s = -18.8$ fm, relevant for neutron matter. Nevertheless, the ladder resummation in the Galitskii integral equation, Eqs. (11) and (12), are supported by dimensional arguments and quantitatively it successfully predicts ν_c between that of neutron and symmetric nuclear matter. The ladder resummation therefore seems to include the most important class of diagrams. However, even small corrections can be important for the magnitude of the gap because they appear in the exponent as, e.g., found for induced interaction [compare Eq. (5) with Eq. (4)]. In addition, superfluidity decreases the energy of the system by $\sim \Delta^2/2E_F$, which can be significant at intermediate densities if gaps really are as large as the Fermi energy.

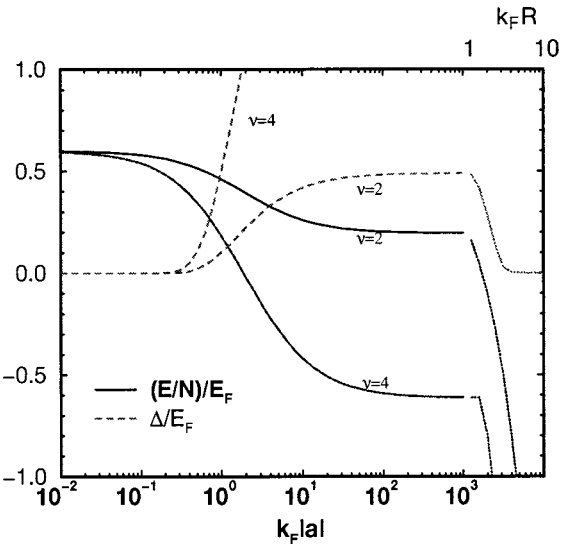

FIG. 1. Ground-state energy and superfluid gaps for a degenerate system of fermions interacting via attractive forces with $R \ll |a|$. The energy per particle E/N [Eq. (11), full curves] and the BCS gap Δ [Eq. (5), dashed curves] are plotted in units of the Fermi energy as function of density for $\nu=2$ and $\nu=4$. Dotted curves to the right show qualitatively the gap and energy per particle at high density (see text) as a function of $k_F R$ (upper axis).

The interesting feature of the intermediate density region, that energies and gaps are independent of the scattering length, leads to the remarkable fact that the system is also insensitive to whether the scattering length goes to plus or minus infinity. In other words, a many particle system is insensitive to whether the two-body system has a marginally bound state just above or below threshold; the two-body bound state or resonance is dissolved in matter at sufficiently high density, $k_F|a| \gtrsim 1$. For positive scattering lengths a pair condensate of molecules may form at low densities but they dissolve at intermediate densities when the range of the two-body wave function exceeds the interparticle distance.

In Fig. 1 the energy per particle is shown as function of density extending from dilute and intermediate densities, Eqs. (7) and (11), to high densities, Eq. (10). At low densities the Fermi kinetic energy dominates but at intermediate densities, $R \lesssim k_F^{-1} \lesssim |a|$, the attractive potential lowers the energy by an amount proportional to the statistical factor. The two cases $\nu=2$ and $\nu=4$ are seen to saturate at positive and negative energies, respectively. In the high-density limit the attractive (Hartree) potential of Eq. (10) dominates and will lead to collapse of all Fermi systems in the absence of repulsive cores.

Figure 1 also shows the superfluid gaps of Eqs. (4) and (5) for dilute and intermediate density Fermi systems. At low densities they decrease exponentially as $\Delta \sim E_F \exp(-2/\pi k_F|a|)$ whereas at intermediate densities the gaps are a finite fraction of the Fermi energy. At high densities the gap generally decreases rapidly with density [15,7]. For example, for an attractive square-well potential of range R and depth V_0 with long scattering length (or marginally bound state), i.e., $V_0 R^2 \simeq \pi^2/4m$, the gap decrease exponentially as $\Delta \sim \exp(-4k_F R/\pi)$. When $|a| \gg R$ plateaus appear for $(E/N)/E_F$ and Δ/E_F. Since E_F also decreases with decreasing density, the gap itself is narrowly peaked near $k_F \simeq 1/R$ as found in nuclear and neutron matter [15].

Information on the density dependence can be obtained independently from calculations within the Wigner-Seitz cell approximation that has recently been employed for the strongly correlated nuclear liquid [16]. The periodic boundary condition is a computational convenience that contains the important scale for nucleon-nucleon correlations given by the interparticle spacing. It naturally gives the correct low-density Eq. (7) and high-density Eq. (10) limits. At intermediate densities one obtains

$$\frac{E}{N} = E_F\left[\frac{3}{5} - c_2\frac{\nu-1}{\nu^{1/3}}\right]. \tag{14}$$

Finite crystal momenta complicates the calculation of c_2. A lower (but reasonable) estimate $c_2 \simeq 0.25$ can be calculated. The potential energy in Eq. (14) is also proportional to the kinetic one as found in Eq. (12) and of similar magnitude. The scaling with $\nu^{-1/3}$ arises because energies scale with the square of the inverse particle spacing, r_0^{-2}, in the Wigner-Seitz cell approximation, and $\rho = \nu k_F^3/6\pi^2 = (4\pi r_0^3/3)^{-1}$; thus $r_0^{-2} \propto \nu^{2/3}$. In addition a factor $(\nu-1)/\nu$ enters because the exchange interaction energy has to be subtracted from the direct. The resulting ν dependence of Eq. (14), differs from the scaling obtained from ladder resummations, Eq. (11), which indicates that the Wigner-Seitz cell approximation is not good enough. The energy per particle can be calculated at all densities and finite values of a and R and the crossover between the three density regimes generally confirm the energy per particle shown in Fig. 1.

For bosons the Wigner-Seitz cell approximation is equivalent to the ''lowest order constrained variational'' method when r_0 is set equal to the healing distance [6]. Consequently, bosons have similar iteraction energies as fermions at intermediate densities $E/N \propto \pm \hbar^2/m r_0^2$, for large positive and negative scattering lengths.

IV. PHASE DIAGRAM

Constructing a phase diagram from the low-temperature degenerate regime to the high-temperature classical regime requires a finite temperature generalization. For illustration we shall follow the procedure as in Ref. [17] and employ the high-temperature approximation for the additional thermal pressure. At high temperatures quantal effects are negligible and the energy per particle is simply given by the classical value $E/N \simeq 3T/2$. The isothermal sound speed is within this approximation

$$s_T^2 = \frac{T}{m} + s_{T=0}^2, \tag{15}$$

where the zero temperature sound speed is given by Eq. (8) with energy per particle from Eqs. (11) and (7). The spinodal instability condition $s_T = 0$, determines the line of collapse $T(\rho)$ for long-wavelength density fluctuations.

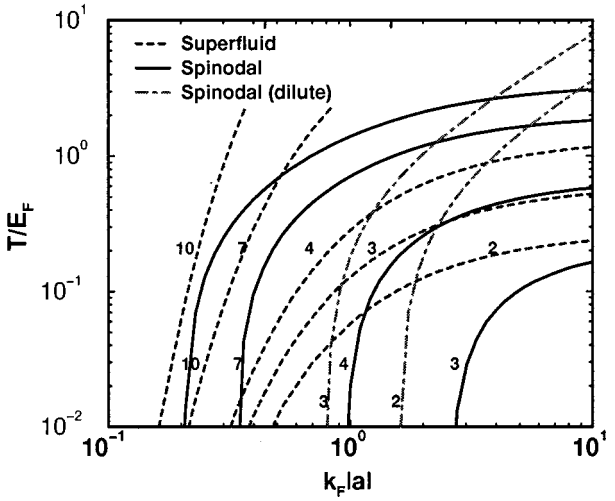

FIG. 2. Phase diagram at low and intermediate densities ($\rho = \nu k_F^3/6\pi$) for a gas of fermions interacting via a long (attractive) scattering length a. Spinodal lines are shown with full curves and the superfluid transition by dashed curves for various numbers of spin states ν, as labeled. The area constrained to the lower-right corner is the spinodally unstable and superfluid region. As systems with two spin states only are stable at intermediate densities, the $\nu=2$ spinodal line is absent. Contrarily, the $\nu=2$ spinodal line based on extrapolating the dilute approximation to higher densities (see text) is shown by dash-dotted curves.

The resulting phase diagram is shown in Fig. 2 for $\nu=2$, 3, 4, 7, and 10 spin states. The lower ($T \lesssim T_F$) and right ($k_F|a| \gtrsim 1$) corner of the phase diagram is the spinodally unstable region where the system collapses. The region decreases for fewer spin states and is absent for $\nu=2$. For comparison the spinodal lines for $\nu=2$ and $\nu=3$ are shown when the dilute approximation of Eq. (7) is extrapolated into intermediate densities. Generally, the spinodally unstable regions based on the dilute approximation are substantially overestimated.

The regions of superfluidity given by $T_c=(\gamma/\pi)\Delta$ and Eq. (5) are also shown in Fig. 2. As for the spinodally unstable region it is the lower-right corner that is superfluid. However, superfluidity extends to lower densities and therefore mechanical instability does not prevent the BCS-type pairing in the case of fermions. The opposite conclusion was reached for the pairing transition in Bose-Einstein condensates [17]. As cooling becomes increasingly difficult at temperatures below the Fermi temperature, we observe that the superfluid transition is readily obtained by increasing the density above $k_F|a| \gtrsim 1$.

The phase diagram is quantitatively correct at low as well as high temperatures. Around the Fermi energy it gives a qualitative description only due to the approximate thermal pressure employed. Furthermore, at intermediate densities, the superfluid gaps become large exceeding the Fermi energy for large spins, and the corrections to the ground-state energies can therefore not be ignored.

Molecular transitions and Efimov states must also be considered at high densities for three and more spin states. Even though two-body bound states do not exist, bound states of three or more particles may exist. Such molecules are also referred to as Efimov states [18]. For two spin states such Efimov ''molecules'' do not exist due to Pauli blocking of the third state and all the results described above therefore apply to Fermion systems with two spin states, e.g., pure neutron matter. Nuclear matter will be unstable towards a molecular transition forming tritum, ^{3}He, helium and heavier nuclei, but as it is also spinodally unstable the two instabilities will compete. This competition applies generally to Fermi systems with four and more spin states. Fermi systems with three spin states may be special because they will be unstable towards forming Efimov states but not necessarily spinodally unstable because $\nu=3$ is marginal as discussed above. Nucleons have the additional feature of the two-body bound-state deuterium, which adds to the possible molecular transitions. Further study of the spinodal and the various molecular collapse time scales is required in order to determined which one is the fastest and thus take place in nature.

V. FINITE SYSTEMS

The degenerate Fermi gases and Bose-Einstein condensates (BEC) produced so far contain $n \sim 10^3 - 10^6$ magnetically trapped alkali atoms. Some of them interact via long scattering lengths such as the triplet ^{6}Li fermions with $a = -2160$ bohrs radii and singlet $^{85}Rb_2$ bosons with $|a| \gtrsim 10^3$ bohrs radii. Large scattering lengths $a \to \pm\infty$ can be taylored by using Feshback resonances, i.e., hyperfine states close to threshold further tuned by magnetic fields. Fermi gases differ from BEC's in several respects. Most importantly, whereas bosons sit at zero-momentum states, fermions have considerable kinetic energy. Therefore, when interactions are small, a BEC has energy per particle $\hbar\omega$ and size a_{osc}, where $\omega=(\omega_\perp \omega_z)^{1/3}$ is the geometric average of the magnetic trap frequencies and $a_{osc}=\hbar/\sqrt{m\omega}$ is the oscillator length. A degenerate gas of N Fermionic atoms has a larger energy per particle $\sim N^{1/3}\hbar\omega$ and size $L \sim N^{1/6} a_{osc}$. In current experiments with degenerate Fermi gases and BEC's the densities are low so that the dilute potential applies and the energy per particle is approximately

$$\frac{E}{N} \simeq \frac{3}{4}\left(\frac{6}{\nu}\right)^{1/3} N^{1/3}\hbar\omega + \frac{\nu-1}{\nu}\frac{2\pi a}{m}\frac{N}{L^3}, \qquad (16)$$

where the average density in the trap has been approximated by $\langle\rho\rangle \simeq N/L^3$ [19]. For a small number of trapped atoms with attractive scattering lengths the system is metastable but for a large number of trapped atoms, $N \gtrsim \nu[a_{osc}/(\nu-1)a]^6$, the attractive potential overcomes the Fermi kinetic energy and the degenerate Fermi gas becomes unstable and implodes. However, around the same density $k_F|a| \gtrsim 1$ and we enter the intermediate density region, where the potential of Eq. (11) should be applied instead of the dilute potential. The gas is therefore mechanically stable for two hyperspins only contrary to conclusions based on the dilute potential [2,20].

A recent experiment on cold magnetically trapped Fermionic atoms [2] observed degeneracy for ^{40}K atoms in the two hyperfine states $m_F=9/2,7/2$. Current experimental oscillator

lengths $a_{osc} \simeq \mu m$ are less than one order of magnitude longer than the atomic scattering length $|a|$ of ^{6}Li. It should be possible to reach intermediate densities, $k_F|a| \gtrsim 1$, by trapping $N \gtrsim 10^6$ ^{6}Li atoms [20]. The atomic gases offer the unique opportunity to vary the densities as well as the relative amount of the hyperfine states. Varying the composition is a convenient way to vary the gaps and attractive potential of Eqs. (7),(11), and (10) through ν for given density and scattering length. In the limit where most atoms are in one of the states, the Fock and Hartree terms almost cancel and effectively $\nu \to 1_+$.

More intricate systems of mixtures of fermions and bosons, e.g., ^{39,40,41}K isotopes can also be studied. If the interaction is attractive it will contract the atomic cloud towards higher densities. Irrespective of whether the bosons or fermions attract or repel, the induced interactions, which are of second order in the fermion-boson coupling, enhance the gap [6].

An artificial ''gravitational'' or ''Coulomb'' force can be exerted on the atoms by shining laser light on the trapped cloud from many directions [21]. It would add an energy per particle of order $\sim GNm^2/L$ to Eq. (16), where G is proportional to the laser field intensity. Such an interaction has several interesting consequences. If G is attractive, it would contract the cloud towards higher densities, which would increase gaps (see also [22]) and for sufficiently large G the intermediate density region is entered. Depending on the strengths and sign of the scattering amplitude and gravitational interactions the kinetic energy of the atoms will be balanced by the magnetic trap and/or the scattering or gravitational interactions. The resulting phase diagram is much more complex.

If such a strong attractive laser field is suddenly applied to the gas, the Jeans instability sets in and the gas collapses until balanced again by the kinetic energy. Subsequently, the system will ''bounce'' analogous to the initial stages of a supernova explosion. If, however, intermediate energies are reached and the number of spins exceed $\nu \gtrsim 2.5$, then the collapse will be further accelerated by the attraction between atoms. The corresponding critical particle number is

$$N_c \simeq (Gm^3 a)^{-3/2}, \tag{17}$$

at zero temperature. It differs from the standard Chandrasekhar mass by a factor $(m|a|)^{3/2}$ because the instability condition is $k_F|a| \simeq 1$, whereas stars go unstable when the particles become relativistic $k_F \simeq m$.

VI. SUMMARY

The energy per particle and superfluid gaps have been calculated for an homogeneous system of fermions interacting via a long attractive s-wave scattering length. In the intermediate region of densities, where the interparticle spacing ($\sim 1/k_F$) is much longer than the range of the interaction but much shorter than the scattering length or $|a|$, the energy per particle and superfluid gaps are proportional to the Fermi energy. The energy per particle increases linearly with the spin-isospin or hyperspin statistical factor such that, e.g., symmetric nuclear matter is unstable in the intermediate density regions and undergoes spinodal decomposition whereas neutron matter and Fermionic atomic gases with few hyperspin states are mechanically stable.

A phase diagram of Fermi gases at low and intermediate densities was constructed by including thermal pressures in the high-temperature classical approximation. With the proper energy per particle at intermediate densities the spinodal region in the phase diagram was reduced substantially as compared to conjectures based on extrapolations from the dilute limit. Generally, mechanical instability does not prevent a superfluid transition for a wide range of densities. This is contrary to Bose gases, where spinodal instabilities exclude pairing transitions [17].

The interaction energies of the many-body system were discussed for magnetically trapped cold degenerate gases of Fermi atoms. In such systems both superfluidity and the intermediate density region should be attainable. In these density regions the superfluid gaps can be large and the stability and sensitivity to the statistical factor ν can be studied. Adding a gravitationally like force by shining laser light on the atomic cloud further increase densities whereby collapse and bounce, analogous to the early stages of supernova explosions may be studied.

ACKNOWLEDGMENTS

Discussions with G. Bertsch, A. Bulgac, V.R. Pandharipande, and C.J. Pethick are gratefully acknowledged.

[1] V. R. Pandharipande, Int. J. Mod. Phys. B **13**, 543 (1999); H. Heiselberg and M. Hjorth-Jensen, Phys. Rep. **328**, 237 (2000).
[2] J. Holland, B. deMarco, and D. S. Jin, e-print cond-mat/9911017; Science **285**, 1703 (1999).
[3] V. M. Galitskii, Zh. Éksp. Teor. Fiz. **34**, 219 (1958) [Sov. Phys. JETP **7**, 151 (1958)].
[4] C. A. R. Sá de Melo, M. Randeria, and J. R. Engelbrecht, Phys. Rev. Lett. **71**, 3202 (1993); H. T. C. Stoof *et al.*, *ibid.* **76**, 10 (1996); T. Papenbrock and C. F. Bertsch, Phys. Rev. C **59**, 2052 (1999).
[5] L. P. Gorkov and T. K. Melik-Barkhudarov, Zh. Éksp. Teor. Fiz. **40**, 1452 (1961) [Sov. Phys. JETP **13**, 1018 (1961)].
[6] H. Heiselberg, C. J. Pethick, H. Smith, and L. Viverit, Phys. Rev. Lett. **85**, 2418 (2000).
[7] Fetter and Walecka, *Quantum Theory of Many Particle Physics* (McGraw-Hill, New York, 1971).
[8] W. Lenz, Z. Phys. **56**, 778 (1929).
[9] K. Huang and C. N. Yang, Phys. Rev. **105**, 767 (1957); T. D. Lee and C. N. Yang, *ibid.* **105**, 1119 (1957).
[10] V. N. Efimov and M. Ya. Amus'ya, Zh. Éksp. Teor. Fiz. **47**, 581 (1964) [Sov. Phys. JETP **20**, 388 (1965)].
[11] V. R. Pandharipande, C. J. Pethick, and V. Thorsson, Phys. Rev. Lett. **75**, 4567 (1995).

[12] K. A. Brueckner, C. A. Levinson, and H. M. Mahmoud, Phys. Rev. **103**, 1353 (1956); H. A. Bethe and J. Goldstone, Proc. R. Soc. London, Ser. A **238**, 551 (1957).
[13] H. Heiselberg, C. J. Pethick, and D. G. Ravenhall, Phys. Rev. Lett. **61**, 818 (1988).
[14] G. A. Baker, Jr., Phys. Rev. C **60**, 054311 (1999).
[15] V. J. Emery and A. M. Sessler, Phys. Rev. **119**, 248 (1960).
[16] J. Carlson, H. Heiselberg, and V. P. Pandharipande, Phys. Rev. C **63**, 017603 (2001).
[17] E. J. Mueller and G. Baym, e-print cond-mat/0005323.
[18] V. N. Efimov, Nucl. Phys. A **210**, 157 (1973).
[19] L. Vichi, M. Inguscio, S. Stringari, and G. M. Tino, J. Phys. B (to be published); e-print cond-mat/9810115.
[20] M. Houbiers *et al.*, Phys. Rev. A **56**, 4864 (1997).
[21] D. O'Dell, S. Giovanazzi, G. Kurizki, and V. M. Akulin, Phys. Rev. Lett. **84**, 5687 (2000).
[22] L. Viverit, S. Giorgini, L. P. Pitaevskii, and S. Stringari, e-print cond-mat/000551.